Revisiting bright δ Scuti stars and their period–luminosity relation with *TESS* and *Gaia* DR3

Natascha Barac[1,2]★, Timothy R. Bedding[2,3]†, Simon J. Murphy[2,3,4] and Daniel R. Hey[2,3,5]
[1]*Department of Physics and Astronomy, University of Pennsylvania, Philadelphia, PA 19104, USA*
[2]*Sydney Institute for Astronomy, School of Physics, University of Sydney, NSW 2006, Sydney, Australia*
[3]*Stellar Astrophysics Centre, Department of Physics and Astronomy, Aarhus University, DK-8000 Aarhus C, Denmark*
[4]*Centre for Astrophysics, University of Southern Queensland, Toowoomba, QLD 4350, Australia*
[5]*Institute for Astronomy, University of Hawai'i, Honolulu, HI, USA*

Accepted 16 April 2019.

ABSTRACT

We have used NASA's TESS mission to study catalogued δ Scuti stars. We examined TESS light curves for 434 stars, including many for which few previous observations exist. We found that 62 are not δ Scuti pulsators, with most instead showing variability from binarity. For the 372 δ Scuti stars, we provide a catalogue of the period and amplitude of the dominant pulsation mode. Using Gaia DR3 parallaxes, we place the stars in the period–luminosity diagram and confirm previous findings that most stars lie on a ridge that corresponds to pulsation in the fundamental radial mode, and that many others fall on a second ridge that is a factor two shorter in period. This second ridge is seen more clearly than before, thanks to the revised periods and distances. We demonstrate the value of the period–luminosity diagram in distinguishing δ Scuti stars from short-period RR Lyrae stars, and we find several new examples of high-frequency δ Scuti stars with regular sequences of overtone modes, including XX Pyx and 29 Cyg. Finally, we revisit the sample of δ Scuti stars observed by Kepler and show that they follow a tight period–density relation.

Key words: parallaxes – stars: variables: delta Scuti – stars: oscillations

1 INTRODUCTION

High-precision photometry from the *Kepler* and *TESS* space missions is revolutionizing the study of pulsating stars (for recent reviews, see Aerts 2021; Kurtz 2022). Combining this photometry with distances measured with Gaia brings new opportunities to investigate period–luminosity (P–L) relations. The P–L relations of classical pulsators have a long history, particularly with Cepheids (Leavitt & Pickering 1912) and RR Lyr variables, making these stars indispensable distance indicators. The P–L relations for their main-sequence cousins—the δ Scuti stars—were studied by McNamara (1997, 2011) using parallaxes from Hipparcos and have recently been revisited using Gaia parallaxes to refine the luminosities (Ziaali et al. 2019; Jayasinghe et al. 2020; Poro et al. 2021; Gaia Collaboration et al. 2022). However, in many cases the catalogued periods were determined decades ago from ground-based photometry. The *TESS* spacecraft is collecting high-precision all-sky photometry, enabling us to measure pulsation periods more precisely and homogeneously than ever before, without atmospheric variability or large daily gaps in the time series.

We have used *TESS* light curves from the first three years of the mission to study catalogued δ Sct stars, including many for which few ground-based observations exist, in order to confirm their status and measure their dominant pulsation modes. We use our revised data, together with Gaia DR3 parallaxes, to place these targets more accurately in the period–luminosity diagram. We build on the work of Ziaali et al. (2019), who used targets from the heterogeneous Rodríguez et al. (2000) catalogue, and fainter stars observed by the *Kepler* mission, to examine the P–L relation for δ Sct stars.

The construction of our sample is described in Sec. 2. Our procedures for analysing *TESS* data and measuring the dominant pulsation mode of each star are outlined in Sec. 3. In Sec. 4 we plot the P–L relation of our sample and outline its value in distinguishing δ Sct stars from other pulsators and from non-pulsating stars. We discuss the excess of stars having a dominant pulsation period that is half that of the predicted fundamental mode (Sec. 4.1), as identified by Ziaali et al. (2019), and also show the period–density relation for *Kepler* δ Sct stars (Sec. 4.2). In Sec. 5, we discuss stars belonging to the class of high-frequency δ Sct stars investigated by Bedding et al. (2020).

2 SAMPLE CONSTRUCTION

Our sample of stars is drawn primarily from the catalogue of Rodríguez et al. (2000, hereafter R2000). In a comprehensive review and compilation of known δ Sct stars (up to January 2000), R2000 catalogued the primary observational properties of 636 stars, including their dominant pulsation periods and visual magnitudes. We only considered the 407 stars with $V < 12$. The *TESS* spacecraft observed 301 stars from this list in its first three years (Sectors 1–39). Of these,

★ E-mail: nbarac@sas.upenn.edu
† E-mail: tim.bedding@sydney.edu.au

194 were observed at 2-min cadence in at least one sector, and the remaining 107 stars only have full-frame image (FFI) data available, which has 30-minute cadence for Sectors 1–26 and 10-minute cadence from Sector 27 onwards. These 302 stars are all included in our sample.

We supplemented our sample with targets from the compilation of 1578 δ Sct stars by Chang et al. (2013, hereafter C2013), which contains 860 δ Sct stars not present in R2000. Of these, we analysed the 133 stars with $V < 12$ that have 2-minute *TESS* data available in Sectors 1–39. Our final sample of 434 stars contains 301 stars from R2000 and 133 additional stars from C2003.

3 PULSATION PERIODS

3.1 *TESS* light curves

We queried the *TESS* data products available on the Mikulski Archive for Space Telescopes (MAST)[1] for each star using the Python Lightkurve package (Lightkurve Collaboration et al. 2018). We downloaded light curves for 2-min targets, whereas for targets with only FFI data we used the Lightkurve wrapper Platypus[2] to extract and correct the time-series data. In both cases, we used all available data from *TESS* Sectors 1–39.

We computed the Fourier transform of each light curve in order to measure the dominant pulsation modes. Due to the non-zero *TESS* integration times, the measured amplitudes are smaller than the intrinsic amplitudes. To account for this averaging, sometimes referred to as 'smearing' or 'apodization', we divided the measured Fourier amplitudes by the function $\mathrm{sinc}\,(\pi\nu t_{\mathrm{int}})$, where t_{int} is the integration time. Because there is no dead time between integrations, this equation can be written as $\mathrm{sinc}\left(\frac{\pi}{2}\frac{\nu}{\nu_{\mathrm{Nyq}}}\right)$, where ν_{Nyq} is the Nyquist frequency (e.g., Huber et al. 2010; Murphy 2012). We note that this correction is more important for the light curves made with 30-min FFI data.

A simple peak-finding algorithm was used to extract the peak with the largest corrected amplitude (i.e. the dominant mode) for each star. This was adequate for our goals, given our focus is identifying δ Sct stars and measuring the dominant modes, rather than carrying out a full frequency analysis on every star. We limited the search to peaks above 3 d^{-1} to capture pressure mode (p-mode) pulsations. Below this limit, pulsation peaks are typically gravity or Rossby modes (e.g., Li et al. 2020).

The period–luminosity relation outlined in Section 3 was also used as a guide to confirm that we were recording the correct pulsation modes. Stars that fell significantly to the right of the P–L relation (that is, those with periods too long to be δ Sct pulsations) were inspected to confirm their variability. A number of these stars were identified as binaries showing no evidence of δ Sct pulsations. Other stars were able to be amended with the correct δ Sct pulsation mode. For example, the highest peak in the spectrum of some stars (e.g., BR Hyi and V353 Tel) was in fact due to binarity, but there were sometimes clear δ Sct pulsations and so the dominant δ Sct mode was manually recorded. These results are compiled in Table 2, which lists the dominant pulsation mode that we have measured in each star from the *TESS* data, along with the corrected amplitude.

[1] https://archive.stsci.edu/
[2] https://github.com/danhey/platypus

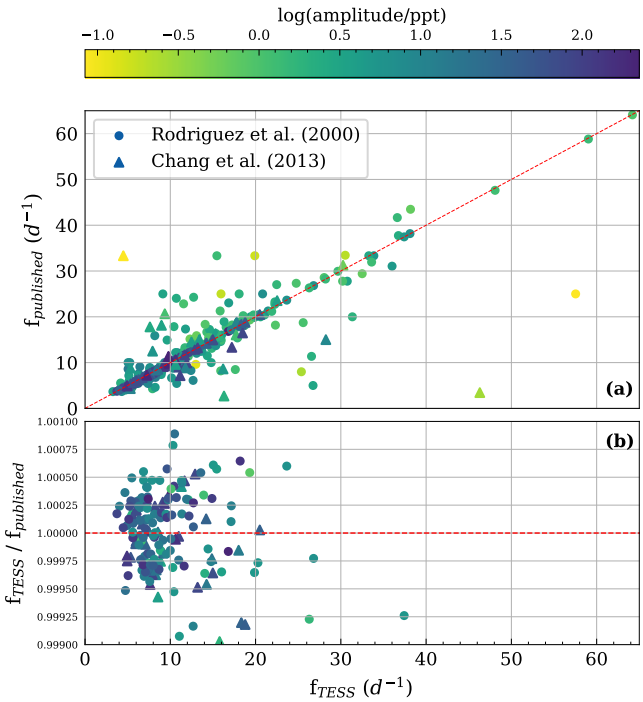

Figure 1. (a) Comparison between the catalogued frequencies and those measured from *TESS*. The red dotted line shows a ratio of 1:1. Stars included in the R2000 catalogue are plotted as circles, while those added from the C2013 catalogue are plotted as triangles. **(b)** Close-up of the ratios of values, highlighting stars whose *TESS*-revised dominant modes are close to their previously published values.

3.2 Non-δ Scuti stars

By inspecting the *TESS* light curves and consulting publications since R2000, we identified 62 stars from our sample that showed no evidence of δ Sct pulsations (see Table 1). Of these, 21 stars were included in the original R2000 catalogue and 41 were added from C2013.

Ziaali et al. (2019) already flagged the following eight stars from R2000 as not having δ Sct pulsations, which we confirmed with *TESS* data:

- V753 Cen, TV Lyn, and UY Cam are RR Lyrae variables (e.g., McNamara 2011; Sneden et al. 2018);
- BQ Phe, DE Oct, and V345 Gem are binaries with no pulsating component (Liakos & Niarchos 2017);
- AK Men was also found to be a binary with no pulsating component; and
- V1228 Cen is a B-type β Cep variable (Pigulski & Pojmański 2008).

Of the 41 stars removed from C2013, several are in binary systems with no pulsating component. Their Fourier spectra often look similar to those of high-amplitude δ Sct stars (HADS) and were initially flagged for inspection after placement in the P–L diagram, for falling outside of the expected area. Finally, HD 229085 shows p-mode pulsations but is too luminous to be a δ Sct star ($M_V = -0.55$); being only 1.0 deg from the Galactic plane, it appears to be a heavily-reddened β Cephei star. Overall, we confirm the value of the P–L relation in helping to identify non-δ Sct pulsators that we might otherwise misclassify.

Table 1. Compilation of 63 stars identified as non-δ Sct stars. Column R2000 is set to 1 for stars listed in Rodríguez et al. (2000), while the remainder are from Chang et al. (2013).

HD	Name	TIC	R2000
2145	BQ Phe	7203984	1
4173	V756 Cas	420842854	0
10088	—	151056397	1
10270	CE Hyi	230983365	1
21102	V1241 Tau	279181220	1
22544	V579 Per	200937303	1
25637	AK Men	394699148	1
43378	UZ Lyn	322679290	0
43601	—	141770299	0
50420	V352 Aur	191999705	1
60987	V345 Gem	4164713	1
77140	FZ Vel	30906332	1
77140	FZ Vel	30906332	0
90747	GS UMa	8245065	1
100495	V1228 Cen	318670307	1
101065	V0816 Cen	163587609	0
106103	GM Com	4738909	0
108662	AI Com	393808105	0
108945	UU Com	393819751	0
109738	—	327436923	0
110411	rho Vir	390607705	0
127986	CP Boo	67993023	0
129723	BP Oct	290356320	0
152896	V645 Her	458574139	0
165373	V831 Her	135362677	0
191747	18 Vul	245152467	1
191803	DE Oct	261459125	1
193084	—	164328483	1
202444	tau Cyg	167092249	0
204420	—	301795154	0
213272	—	100601011	1
213272	—	100601011	0
229085	—	13332837	0
271923		41232835	0
289243	V0783 Mon	237554493	0
302013	V753 Cen	300892362	1
339669	V382 Vul	245236103	1
343341	V1003 Her	282137421	1
—	TU UMi	257002707	1
—	TV Lyn	157798407	1
—	UY Cam	441619744	1
—	V705 Per	101256059	0
—	—	25671619	0
—	—	34137913	0
—	—	35166984	0
—	—	41994216	0
—	—	60657338	0
—	—	70870736	0
—	—	73764693	0
—	—	78002882	0
—	—	138735041	0
—	—	152288704	0
—	—	152359020	0
—	—	185259483	0
—	—	238170857	0
—	—	248348545	0
—	—	270709500	0
—	—	335826251	0
—	—	383604347	0
—	—	396424970	0
—	—	410299018	0
—	—	421452112	0

3.3 Comparison with published periods

Figure 1 compares the dominant pulsation mode recorded in the original catalogues with our values from *TESS*. The values agree well for the majority of our sample: periods for 67 percent of the stars are within 10% of the original value. It appears that stars with larger differences are primarily those with amplitudes smaller than 1 mmag. This is presumably a result of lower signal-to-noise ratio and poorer time coverage of the ground-based observations, making it difficult to accurately identify and measure the dominant mode. Some δ Sct stars are also known to undergo amplitude modulation (see Bowman et al. 2016, and references therein), which may have caused a new mode to become dominant since the previous studies.

4 PERIOD–LUMINOSITY RELATION

Revising the dominant modes of our sample allows them to be placed more accurately in the period–luminosity diagram. We calculated the absolute V-band magnitudes (M_V) for these stars using:

$$M_V = V + 5\log_{10}\pi + 5 - A_V, \quad (1)$$

where π is the parallax in arcsec. We used parallaxes from *Gaia* DR3, except in the cases where the parallax from *Hipparcos* was more precise. The extinction due to interstellar dust (A_V) was calculated by fitting the spectral energy distribution (SED) of each star using the astroARIADNE[3] python package. For each star, we queried photometric data from the Vizier database (Ochsenbein et al. 2000). The stars were then fitted to the Castelli & Kurucz (2003) model using a nested sampling algorithm (dynesty, Speagle 2020) to obtain extinctions. In order to obtain a uniform sample of apparent (V) magnitudes, we used Tycho V_T and B_T magnitudes converted to the Johnson V photometric system using the linear transformation

$$V = V_T - 0.090(B_T - V_T), \quad (2)$$

for which systematic errors do not exceed 0.015 magnitudes (ESA 1997). In plotting, we further limited our sample to stars with fractional parallax uncertainties < 5%, and extinction $A_V < 0.2$.

Figure 2 shows our updated period–luminosity relation, colour-coded by pulsation amplitude. The red crosses show RR Lyrae variables, which have their own P–L relation (McNamara 2011; Sneden et al. 2018; Molnár et al. 2022; Garofalo et al. 2022). Indeed, when accurate parallaxes are available, the P–L diagram is a useful way to distinguish between HADS and short-period RR Lyr variables (so-called RRc stars, which pulsate in the first overtone), whose light curves look very similar. The dashed red line in Fig. 2 is the P–L relation fitted by Ziaali et al. (2019),

$$M_V = (-2.94 \pm 0.06)\log(P/\mathrm{d}) - (1.34 \pm 0.06), \quad (3)$$

which was based on periods from R2000 and parallaxes from Gaia DR2. This result is similar to the P–L relation derived by McNamara (2011), which was fitted to HADS stars thought to pulsate in their fundamental radial mode. We have performed a new fit using our revised measurements, which gives a slightly steeper P–L relation:

$$M_V = (-3.01 \pm 0.07)\log(P/\mathrm{d}) - (1.40 \pm 0.07). \quad (4)$$

This updated relation is show as the solid black line in Fig. 2.

We see in Fig. 2 that higher-amplitude stars tend to fall closer to the fundamental-mode ridge, while lower-amplitude stars show more scatter. This main ridge is also sharper than that of Ziaali et al.

[3] https://github.com/jvines/astroARIADNE

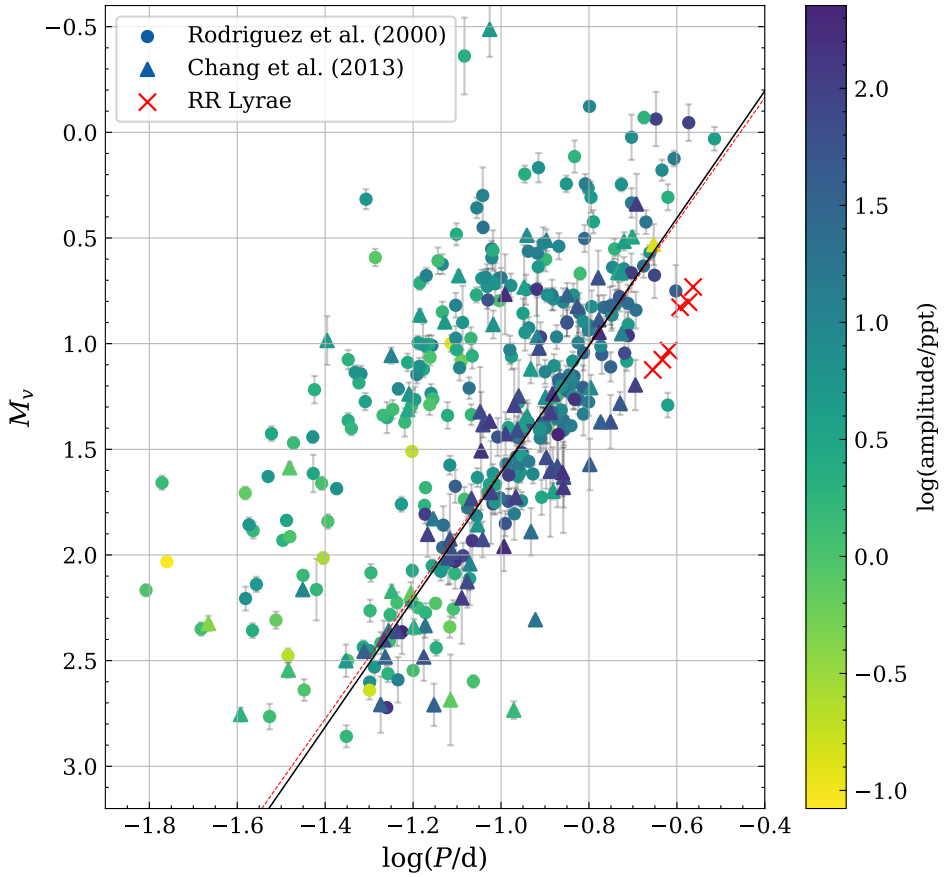

Figure 2. Period–luminosity diagram of δ Sct sample, using periods from *TESS* data and distances from Gaia DR3. The stars plotted are restricted to variables having apparent V magnitudes brighter than 12.0, and fractional parallax uncertainties less than 5 percent. The dashed red line is the P–L relation fitted by Ziaali et al. (2019) and the solid black line is our revised relation (Eq. 4).

(2019), and there are fewer stars falling to the lower right of the relation. Using our revised periods and distances has also made the second ridge, lying to the left of the fundamental-mode ridge, more distinct than before.

Figure 3 shows the horizontal distance of data points to Eq. 4 as a histogram. We confirm a strong excess of stars displaced to the left by 0.30 in log P, corresponding to a period ratio of 0.50. Since histogram results can depend on bin size, we also added a fixed-bandwidth kernel density estimate (KDE; Terrell & Scott 1992) for the same data to Fig. 3. The excess of stars displaced to the left of 0.3 in log P is still present in the KDE, lending support that the excess seen in the histogram is real.

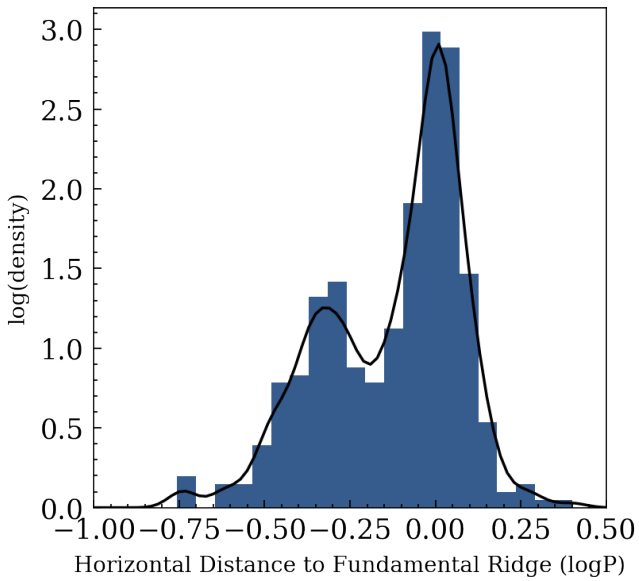

Figure 3. Histogram showing the horizontal distance of data points to the P–L relation in Eq. 4, overlaid with a fixed-bandwidth kernel density estimate (KDE) highlighting the same excess of stars displaced by −0.3 in log P from the fundamental mode ridge.

4.1 Second Ridge Stars

The excess of second-ridge stars was identified by Ziaali et al. (2019) but has not yet been explained. Figure 4 shows the amplitude spectra of the 48 stars whose horizontal displacement in log P from the main ridge falls in the range −0.35 to −0.25. In many cases, we can see a peak at half the frequency of the highest peaks, corresponding to the expected position of the fundamental mode. Conversely, some stars appear to only coincidentally lie on the second ridge. These are typical δ Sct and even HADS that are displaced, perhaps due to binarity or some other error in their absolute magnitudes.

We note, for example, the following stars that appear to be shifted vertically in absolute magnitude due to binarity:

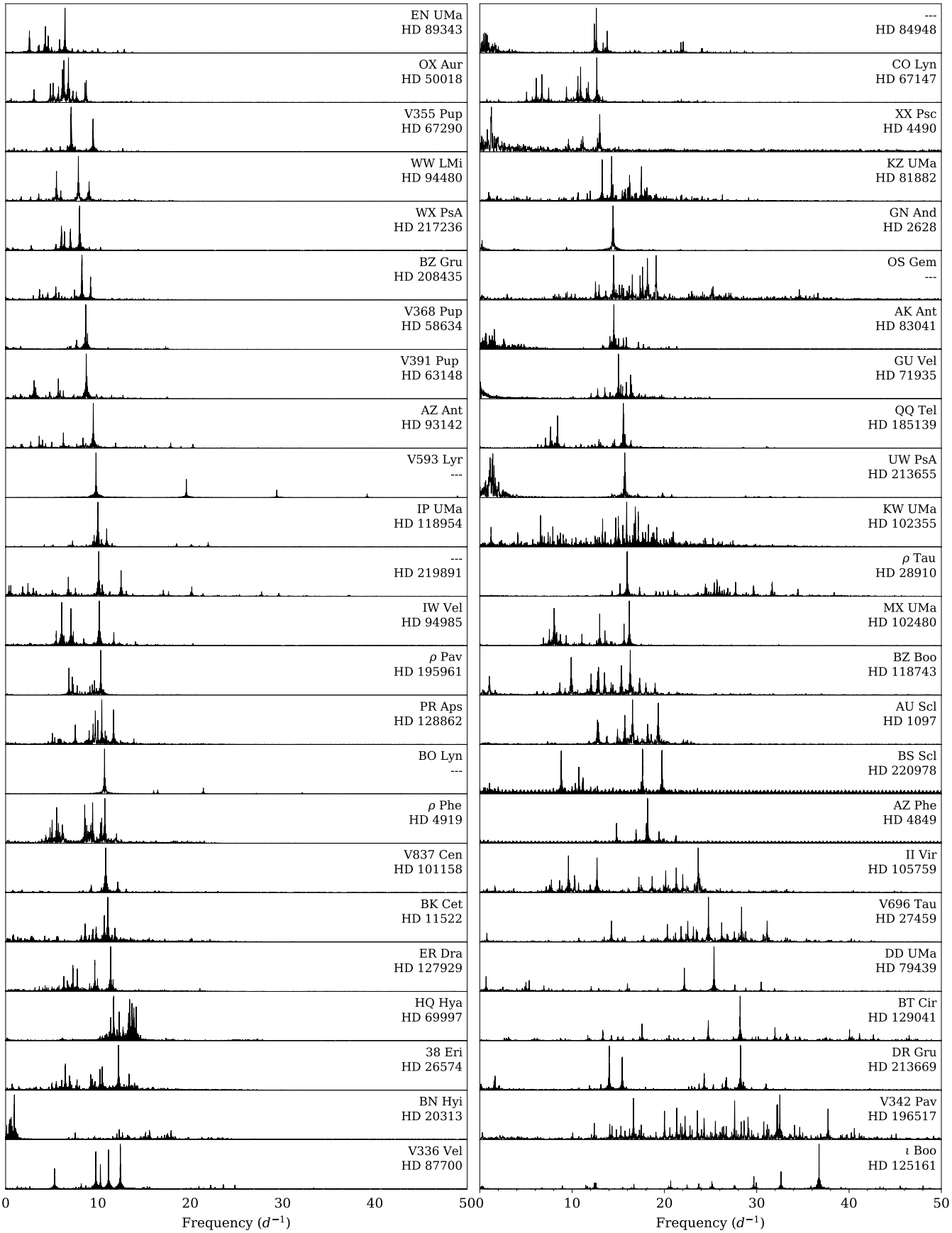

Figure 4. Pulsation spectra of the 48 δ Sct stars lying on the second ridge of our Period–Luminosity diagram, ordered by increasing frequency of the dominant pulsation mode. The vertical axis is amplitude in normalized units.

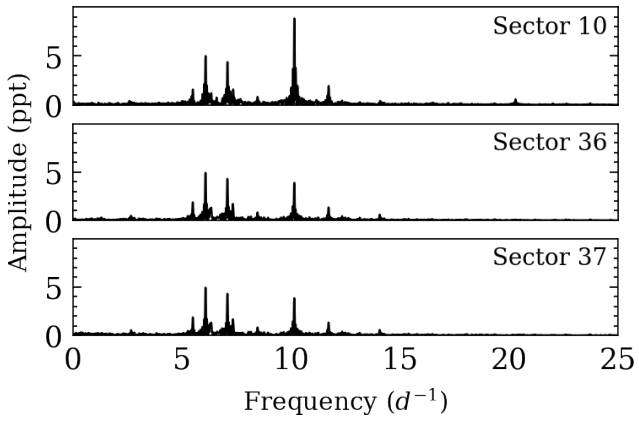

Figure 5. Pulsation spectra of IW Vel, a second-ridge star that shows changes in amplitude over time (see Sec. 4.1).

- BO Lyn looks like a typical HADS with main peak at 10.71 (60 ppt), plus weaker peaks at 16.47 (5 ppt) and 16.04 (4 ppt). We suspected it to be a binary, and therefore vertically displaced in absolute magnitude, as the dominant mode of HADS should fall on the fundamental-mode P–L sequence. Indeed, Li et al. (2018) suggested it has an A-type companion in a 35-yr orbit, based on variations in the pulsation phase over the past century.
- ρ Tau (HD 28910) is a member of the Hyades, with a Hipparcos parallax of 20.61 mas which matches the cluster. It lies above the cluster isochrone in the colour–magnitude diagram, and Antonello & Pasinetti Fracassini (1998) suggest it is a binary. Hence, it is probably shifted up and not a true second-ridge star.
- RS Cha (9 Cha; HD 75747; not shown in Fig. 4 because its horizontal displacement is −0.23) is a contact EB consisting of two pre-main-sequence stars with tidally perturbed pulsations (Steindl et al. 2021). Since these stars have similar luminosities, our absolute magnitude is too bright by about 0.7 and has shifted the star towards the second ridge.

These exceptions are few: the majority of stars on the second ridge are not binaries. Furthermore, we confirm the finding by Ziaali et al. (2019) that known binary systems do not lie preferentially on the second ridge.

An alternative explanation may come from amplitude modulation and mode resonances. We have discussed amplitude modulation on the timescales of decades as contributing to changes between the measurements from our source catalogues (R2000 or C2013), and *TESS* measurements of the dominant pulsation mode. While the timescales of continuous *TESS* observations of our sample are too small to conduct a complete analysis of amplitude modulation, a number of stars in our sample have *TESS* observations separated by a year or more. Interestingly, of these, several second ridge stars show modulation of the second-ridge mode between observations, so that the fundamental radial mode becomes the dominant mode.

IW Vel (HD 94985) is one such example. IW Vel was observed by *TESS* in Sector 10 in 2019, and again in Sectors 36 and 37 in 2021. Figure 5 shows clear amplitude modulation of the second ridge mode ($10.15\,d^{-1}$) between Sectors 10 and 36, two years apart, continuing to Sector 37. In total, the amplitude drops by 67 percent between Sectors 10 and 37, with a 25 percent decrease occurring between Sectors 36 and 37. This moves IW Vel off the second ridge.

Similarly, BS Scl was observed by *TESS* in Sector 2 in 2018, and again in Sector 29 in 2020. In Sector 2, the second ridge mode at $17.63\,d^{-1}$ is dominant with an amplitude of 1.38 ppt, while the fundamental radial mode peak at $8.83\,d^{-1}$ has an amplitude of 1.29 ppt. By Sector 29 however, the second ridge mode has decreased in amplitude by 27 percent and is no longer the dominant frequency. We also note that the peak at $11.2\,d^{-1}$ undergoes significant modulation, decreasing in amplitude by about 42 percent.

In summary, it is possible that stars occupy the second ridge only temporarily, perhaps when a mode of higher radial order is boosted to a higher amplitude through interactions with other modes.

Finally, we note that the amplitude spectrum of HQ Hya (Fig. 4) is similar to those of a new class of δ Sct stars that have been identified in *Kepler* data (see Fig. B12 of Murphy et al. 2019). These stars are characterised by a broad power excess containing many closely spaced peaks, rather than the more widely separated peaks that are seen in most δ Sct stars. We are not aware of an explanation of this phenomenon but we have noticed several other examples in our sample (e.g., BG Hyi, AI Scl, VV Ari and 60 Tau = V775 Tau).

4.2 Period–density relation of the *Kepler* δ Scuti sample

There have been numerous studies of the several thousand δ Sct stars observed by the *Kepler* Mission (for reviews, see Guzik 2021; Kurtz 2022). Here, we take advantage of the Gaia parallaxes to investigate their period–density relation. There is a well-established relationship between the period of a pulsating star and its mean density (e.g., Catelan & Smith 2015, sec. 5.2). The relation is usually written as

$$P = Q \left(\frac{\rho}{\rho_\odot} \right)^{-0.5} , \tag{5}$$

where the pulsation constant, Q, has a different value for each mode.[4] For the fundamental radial mode in δ Sct stars, Q is about 0.033 d (e.g., Fitch 1981; North et al. 1997; Breger 2000; Lovekin & Guzik 2017).

Calculating densities for a large number of stars requires estimating masses by fitting evolutionary tracks in the H–R diagram. This has been done using Gaia DR2 parallaxes for the full set of *Kepler* targets by Berger et al. (2020) and we used their masses and radii to estimate densities the *Kepler* δ Sct stars. Figure 6 show the period–density relation, where period of the dominant mode in each star was taken from Murphy et al. (2019). The diagram looks very similar to the period–luminosity relation (Ziaali et al. 2019) but with the vertical axis reversed, which is expected because of the tight inverse correlation between luminosity and density. Most points in Fig. 6 lie on a ridge that corresponds to the radial fundamental mode. This is confirmed by the dashed line, which shows the theoretical relation (Eq. 5) with $Q = 0.0315$ d. We also see clearly the excess of points on the second ridge, with half this period.

5 HIGH-FREQUENCY δ SCUTI STARS

Some of the stars in our sample belong to the class of high-frequency δ Sct stars, discovered by Bedding et al. (2020) to have remarkably regular sequences of overtone modes. Three were listed in that paper, namely EX Eri (HD 30422), V435 Car (HD 44958) and V349 Pup (HD 59594), but only for V435 Car was the échelle diagram shown.

[4] Note that Eq. 5 applies to pressure modes (p modes), which include pulsations in δ Scuti stars, β Cephei stars and solar-like oscillators. It does not apply to gravity modes (g modes), such as those in γ Doradus stars, Slowly Pulsating B stars and white dwarfs.

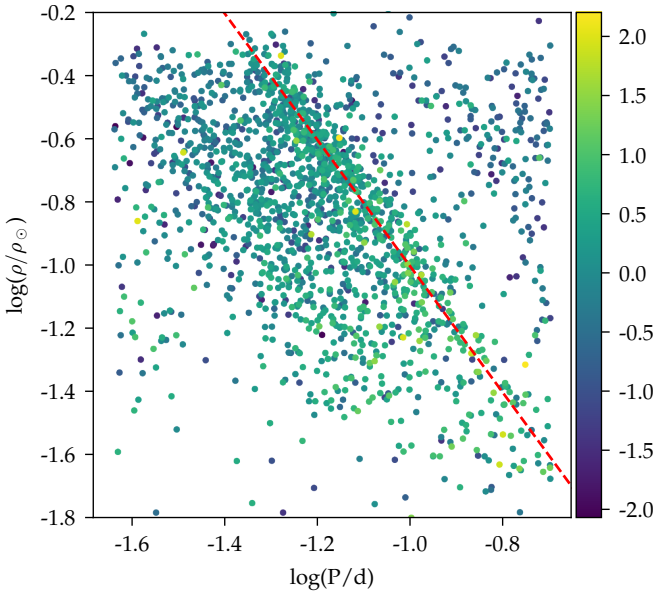

Figure 6. Period–density relation for *Kepler* δ Sct stars. Points show the dominant pulsation mode in each star, colour-coded by the logarithm of the pulsation amplitude in ppt. Pulsation periods and amplitudes were taken from Murphy et al. (2019) and densities were calculated from the *Kepler Stellar Properties Catalog* (Berger et al. 2020). The red dashed line shows the theoretical period–density relation (Eq. 5) with a pulsation constant of $Q = 0.0315$ d. Points in the upper right are γ Dor stars (see Ziaali et al. 2019).

The échelle diagram for EX Eri was shown by Murphy et al. (2020), who also showed échelle diagrams for four other stars in our sample: V1023 Cen (HD 102541), MO Hya (HD 111786), V346 Pav (HD 168740) and HD 210111. We show two more examples, XX Pyx and 29 Cyg, in the next sections. It is noteworthy that in many high-frequency δ Sct stars, the fundamental mode is not the strongest mode (Bedding et al. 2020). Such is the case for all five Pleiades δ Sct stars with *Kepler*-K2 data that were recently studied by Murphy et al. (2022).

5.1 XX Pyx

XX Pyx is a multi-periodic pulsator that has been the subject of three ground-based multi-site campaigns (Handler et al. 2000, and references therein). The star was not observed by *TESS* in Cycle 1 because it fell in a gap between fields, but it was observed in Cycle 3 (Sector 35). The *TESS* light curve (Fig. 7) confirms that it is an ellipsoidal variable with a binary period of 1.15 d, as found by Aerts et al. (2002).

Handler et al. (2000) detected 19 independent pulsation frequencies in the range 27–38 d^{-1}, and suggested a large separation of 4.63 d^{-1}. By generating an échelle diagram with those frequencies, Bedding et al. (2020) confirmed that a value of $\Delta\nu = 4.70\,\mathrm{d}^{-1}$ gave a reasonably good alignment of the peaks. Figure 7 shows the *TESS* amplitude spectrum in échelle format. We confirm that $\Delta\nu = 4.68\,\mathrm{d}^{-1}$ produces a ridge on the left-hand-side that we can identify as $l = 1$ modes (see Bedding et al. 2020 for discussion of similar stars). Three of these modes were detected by Handler et al. (2000), and we see two additional weaker $l = 1$ modes in this ridge. This star is clearly worthy of further study.

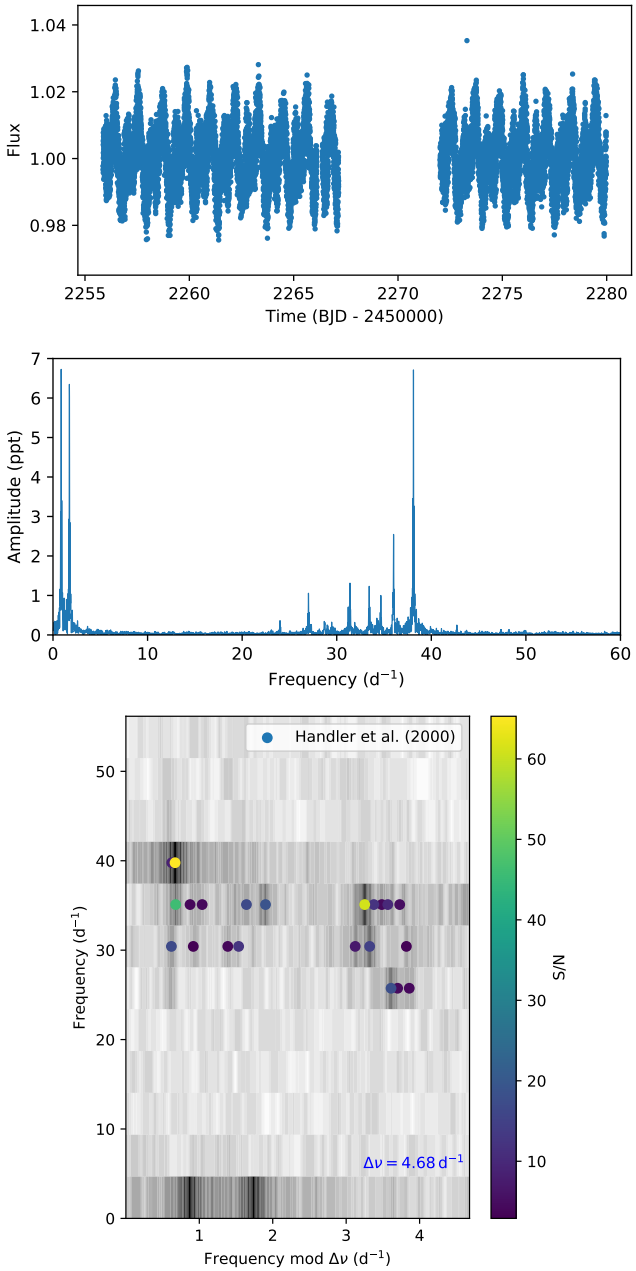

Figure 7. *TESS* observations of XX Pyx (Sector 35), showing the light curve (top), the amplitude spectrum (middle), and the amplitude spectrum in échelle format. The circles in the échelle diagram show the frequencies reported by Handler et al. (2000), colour-coded by signal-to-noise (their Table 4).

5.2 29 Cyg

29 Cyg (V1644 Cyg; HD 192640) is a multi-periodic pulsator that has been the subject of two ground-based multi-site campaigns by Mkrtichian et al. (2007). They measured 11 modes in the range 20–37 d^{-1} and suggested a large separation of $\Delta\nu = 4.82\,\mathrm{d}^{-1}$. Theoretical models using these frequencies were calculated by Casas et al. (2009). The *TESS* data, shown in Fig. 8, confirm that 29 Cyg is a high-frequency δ Sct star with a large separation of $\Delta\nu = 4.85\,\mathrm{d}^{-1}$. With a magnitude of $V = 4.9$, this makes 29 Cyg the brightest known member of this class of stars and an ideal target for follow-up obser-

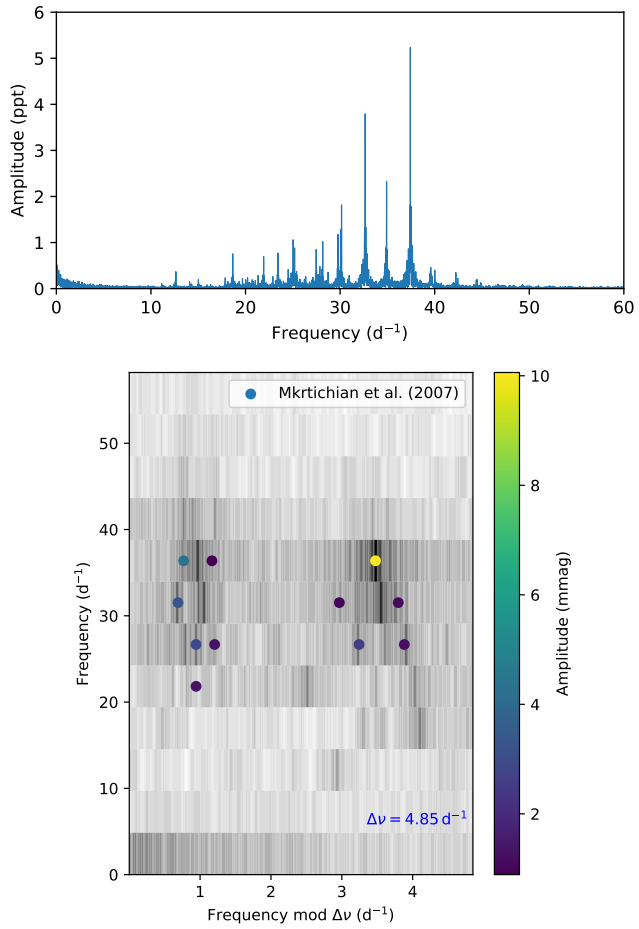

Figure 8. *TESS* observations of 29 Cyg (Sectors 14 and 15), showing the amplitude spectrum (top), and the échelle diagram (bottom). The circles show the frequencies reported by Mkrtichian et al. (2007), colour-coded by amplitude (their Table 8).

vations. It is also known to be a λ Boo star, which is common among high-frequency δ Sct stars (Bedding et al. 2020; Murphy et al. 2020).

6 CONCLUSIONS

We have examined 434 stars observed by the *TESS* mission, drawn from the catalogues of δ Sct stars by Rodríguez et al. (2000) and Chang et al. (2013). We found that 62 are not δ Sct pulsators, with most instead showing variability from binarity. For each of the 372 δ Sct stars, we measured the frequency and amplitude of their strongest pulsation mode. Using Gaia DR3 parallaxes, we placed the stars in the period–luminosity diagram (Fig. 2), in which most stars lie on a ridge that corresponds to pulsation in the fundamental radial mode. We showed the value of the period–luminosity diagram in distinguishing δ Scuti stars from short-period RR Lyrae stars. We also confirmed the findings of Ziaali et al. (2019) that many stars fall on a second ridge that is a factor two shorter in period. This second ridge is seen more clearly than before, thanks for the revised periods and distances. Given that several stars falling on this ridge undergo amplitude modulation on timescales of years, this may signify energy transfer between modes and suggests a transient nature to a star's occupation of the second ridge.

Using densities published by Berger et al. (2020), we show that the δ Scuti stars observed by *Kepler* follow a tight period–density relation, with a pulsation constant for the fundamental mode of Q = 0.0315 d. Finally, we discuss several new examples of high-frequency δ Scuti stars with regular sequences of overtone modes, including XX Pyx and 29 Cyg.

ACKNOWLEDGEMENTS

We gratefully acknowledge support from the Australian Research Council through DECRA grant DE180101104, Future Fellowship FT210100485, and Discovery Project DP210103119, and from the Danish National Research Foundation (Grant DNRF106) through its funding for the Stellar Astrophysics Center (SAC). This work has made use of data from the European Space Agency (ESA) mission *Gaia*, (`https://www.cosmos.esa.int/gaia`), processed by the *Gaia* Data Processing and Analysis Consortium (DPAC, `https://www.cosmos.esa.int/web/gaia/dpac/consortium`). Funding for the DPAC has been provided by national institutions, in particular the institutions participating in the *Gaia* Multilateral Agreement. We are grateful to the entire Gaia and *Kepler* teams for providing the data used in this paper. We also thank László Molnár for useful discussions on RR Lyrae stars.

REFERENCES

Aerts C., 2021, Reviews of Modern Physics, 93, 015001
Aerts C., Handler G., Arentoft T., Vandenbussche B., Medupe R., Sterken C., 2002, MNRAS, 333, L35
Antonello E., Pasinetti Fracassini L. E., 1998, A&A, 331, 995
Bedding T. R., et al., 2020, Nature, 581, 147
Berger T. A., Huber D., van Saders J. L., Gaidos E., Tayar J., Kraus A. L., 2020, AJ, 159, 280
Bowman D. M., Kurtz D. W., Breger M., Murphy S. J., Holdsworth D. L., 2016, MNRAS, 460, 1970
Breger M., 2000, in ASP Conf. Series, Vol. 210. p. 3
Casas R., Moya A., Suárez J. C., Martín-Ruíz S., Amado P. J., Rodríguez-López C., Garrido R., 2009, ApJ, 697, 522
Castelli F., Kurucz R. L., 2003, in Piskunov N., Weiss W. W., Gray D. F., eds, IAU Symposium Vol. 210, Modelling of Stellar Atmospheres. p. A20 (`arXiv:astro-ph/0405087`)
Catelan M., Smith H. A., 2015, Pulsating Stars. Wiley-VCH, Weinheim, Germany
Chang S. W., Protopapas P., Kim D. W., Byun Y. I., 2013, AJ, 145, 132
ESA 1997, The HIPPARCOS and TYCHO catalogues. Astrometric and photometric star catalogues derived from the ESA HIPPARCOS Space Astrometry Mission. ESA Special Publication Vol. 1200, ESA Publications Division, Noordwijk, Netherlands
Fitch W. S., 1981, ApJ, 249, 218
Gaia Collaboration et al., 2022, arXiv e-prints, p. arXiv:2206.06075
Garofalo A., Delgado H. E., Sarro L. M., Clementini G., Muraveva T., Marconi M., Ripepi V., 2022, arXiv e-prints, p. arXiv:2203.07435
Guzik J. A., 2021, Frontiers in Astronomy and Space Sciences, 8, 55
Handler G., et al., 2000, MNRAS, 318, 511
Huber D., et al., 2010, ApJ, 723, 1607
Jayasinghe T., et al., 2020, MNRAS, 493, 4186
Kurtz D., 2022, arXiv e-prints, p. arXiv:2201.11629
Leavitt H. S., Pickering E. C., 1912, Harvard College Observatory Circular, 173, 1
Li L.-J., Qian S.-B., Zhang J., Zhu L.-Y., Liao W.-P., 2018, Research in Astronomy and Astrophysics, 18, 011
Li G., Van Reeth T., Bedding T. R., Murphy S. J., Antoci V., Ouazzani R.-M., Barbara N. H., 2020, MNRAS, 491, 3586
Liakos A., Niarchos P., 2017, MNRAS, 465, 1181

Lightkurve Collaboration et al., 2018, Lightkurve: Kepler and TESS time series analysis in Python, Astrophysics Source Code Library (ascl:1812.013)
Lovekin C. C., Guzik J. A., 2017, ApJ, 849, 38
McNamara D., 1997, PASP, 109, 1221
McNamara D. H., 2011, AJ, 142, 110
Mkrtichian D. E., et al., 2007, AJ, 134, 1713
Molnár L., et al., 2022, ApJS, 258, 8
Murphy S. J., 2012, MNRAS, 422, 665
Murphy S. J., Hey D., Van Reeth T., Bedding T. R., 2019, MNRAS, 485, 2380
Murphy S. J., Paunzen E., Bedding T. R., Walczak P., Huber D., 2020, MNRAS, 495, 1888
Murphy S. J., Bedding T. R., White T. R., Li Y., Hey D., Reese D., Joyce M., 2022, MNRAS, 511, 5718
North P., Jaschek C., Egret D., 1997, in Bonnet R. M., et al., eds, ESA Special Publication Vol. 402, Hipparcos – Venice '97. p. 367
Ochsenbein F., Bauer P., Marcout J., 2000, A&AS, 143, 23
Pigulski A., Pojmański G., 2008, A&A, 477, 907
Poro A., et al., 2021, PASP, 133, 084201
Rodríguez E., López-González M. J., López de Coca P., 2000, A&AS, 144, 469
Sneden C., et al., 2018, AJ, 155, 45
Speagle J. S., 2020, MNRAS, 493, 3132
Steindl T., Zwintz K., Bowman D. M., 2021, A&A, 645, A119
Terrell G. R., Scott D. W., 1992, The Annals of Statistics, 20, 1236
Ziaali E., Bedding T. R., Murphy S. J., Van Reeth T., Hey D. R., 2019, MNRAS, 486, 4348

Table 2: Properties of 372 δ Sct stars in our sample. Column R2000 is set to 1 for stars listed in Rodríguez et al. (2000), while the remainder are from Chang et al. (2013); $f_{\rm cat}$ is the published dominant frequency; f_1 and a_1 are the frequency and amplitude of the dominant frequency we measured with *TESS*; the remaining columns were calculated as described in Sec. 4.

HD	Name	TIC	R2000	$f_{\rm cat}$	f_1	a_1	dist	e_dist	A_V	e_A_V	M_V	e_M_V
				d^{-1}	d^{-1}	ppt	pc	pc	mag	mag	mag	mag
205	V1026 Cas	359127550	0	—	6.25	0.01	307.96	1.16	0.10	0.06	1.21	0.06
1097	AU Scl	12473170	1	17.73	16.55	0.00	325.34	5.44	0.13	0.05	1.37	0.07
1479	V377 Cas	327585336	1	33.33	15.46	0.00	—	—	0.00	0.00	2.25	0.00
2628	GN And	440665786	1	14.43	14.43	0.01	61.23	0.54	0.05	0.04	1.24	0.04
2724	BB Phe	116157537	1	5.74	6.16	0.00	134.51	0.38	0.11	0.05	0.42	0.05
3112	tet Tuc	38847248	1	20.28	20.28	0.01	139.98	0.44	0.07	0.05	0.32	0.05
3326	BG Cet	98660068	1	33.44	30.52	0.00	50.66	0.09	0.06	0.03	2.48	0.03
4490	XX Psc	435860104	1	9.62	12.99	0.00	102.20	0.28	0.06	0.04	1.00	0.04
4494	CN Phe	80432574	1	14.29	12.83	0.00	266.09	1.22	0.07	0.03	2.26	0.04
4849	AZ Phe	80474886	1	18.15	18.17	0.00	97.06	0.63	0.20	0.07	1.35	0.07
4919	ρ Phe	369666165	1	5.45	10.75	0.01	75.00	0.29	0.13	0.10	0.73	0.11
6667	—	248345301	0	18.02	18.02	0.01	255.76	6.46	0.06	0.05	2.36	0.07
6859	V361 And	186297798	1	8.76	8.77	0.01	238.84	1.45	0.11	0.07	0.74	0.07
6870	BS Tuc	234548714	1	15.38	17.87	0.00	107.55	0.19	0.04	0.03	2.28	0.03
7312	AI Scl	183595451	1	24.04	10.71	0.00	68.68	0.11	0.06	0.04	1.70	0.04
8511	AV Cet	10838265	1	14.60	15.91	0.00	66.25	0.13	0.04	0.03	2.07	0.03
8781	BG Hyi	52258534	1	8.96	9.04	0.00	186.10	0.47	0.11	0.05	1.61	0.05
8801	V529 And	189381343	0	20.66	9.36	0.00	53.30	0.00	0.06	0.04	2.73	0.04
9065	WZ Scl	70489756	1	10.43	10.42	0.01	93.51	0.21	0.12	0.04	1.61	0.04
9100	VX Psc	381320713	1	7.35	6.34	0.01	138.79	0.61	0.05	0.04	0.26	0.04
9133	XX Scl	70490868	1	20.45	20.36	0.00	334.22	6.03	0.02	0.02	1.27	0.04
9800	V365 And	308719469	1	7.00	7.00	0.01	168.37	0.53	0.11	0.07	1.15	0.08
10845	VY Psc	88773937	1	4.57	5.51	0.00	154.27	0.40	0.05	0.04	0.55	0.05
11285	VV Ari	91277922	1	13.09	12.63	0.00	168.27	1.07	0.10	0.05	0.48	0.05
11413	BD Phe	229150702	1	26.81	26.80	0.01	78.04	0.17	0.03	0.03	1.44	0.03
11522	BK Cet	92984630	1	11.07	11.06	0.00	101.36	0.32	0.07	0.04	0.69	0.04
11667	—	229154157	0	10.99	10.99	0.08	457.77	2.32	0.06	0.05	1.38	0.06
11956	FG Eri	231048083	1	6.29	6.29	0.01	230.32	0.91	0.03	0.02	-0.12	0.02
12389	—	63395663	1	25.00	20.83	0.01	229.70	2.23	0.03	0.03	1.14	0.04
12743	V373 And	184589181	1	8.87	9.24	0.01	153.77	0.49	0.10	0.05	1.54	0.05
13079	V419 And	184679514	1	20.00	19.41	0.00	181.74	0.64	0.08	0.06	2.53	0.06
13122	V784 Cas	12221925	1	9.16	9.16	0.02	98.18	0.27	0.10	0.06	1.58	0.06
13755	CV Phe	7245720	0	12.50	7.93	0.01	200.20	0.65	0.08	0.05	1.25	0.05
15634	TY For	120932152	1	10.30	10.30	0.00	91.93	0.85	0.04	0.04	1.67	0.04
16189	DX Cet	278962831	1	9.62	9.62	0.05	109.16	0.32	0.07	0.06	1.75	0.06
16439	V663 Cas	280129361	1	17.12	17.13	0.01	309.04	1.52	0.03	0.02	1.21	0.03
16698	FI Eri	142266756	1	5.84	5.84	0.03	324.29	3.10	0.08	0.05	0.83	0.06
16723	BS Cet	441131892	1	8.93	7.61	0.01	147.60	0.50	0.07	0.05	0.79	0.05
17138	RZ Cas	302771290	1	64.10	64.20	0.00	65.31	0.10	0.03	0.02	2.17	0.03
17892	V579 Per	67712263	1	20.24	18.55	0.00	—	—	0.00	0.00	1.34	0.01
17978	VV For	65484200	1	17.33	11.78	0.00	324.82	1.89	0.05	0.04	2.11	0.05
18655	—	365225836	0	14.88	14.88	0.02	283.54	1.74	0.07	0.05	2.33	0.06
18878	V509 Per	192374290	1	6.86	6.87	0.01	115.94	0.35	0.07	0.04	1.08	0.05
19279	V521 Per	192533869	1	14.45	14.85	0.00	86.13	0.25	0.02	0.02	1.68	0.02
20313	BN Hyi	348762920	1	15.15	12.31	0.00	80.27	0.28	0.07	0.05	1.08	0.05
20429	AR Ari	28833184	1	5.65	5.15	0.02	239.09	2.01	0.11	0.09	0.81	0.09
20919	V461 Per	252829836	1	28.57	28.04	0.00	181.26	1.07	0.09	0.04	2.64	0.05
21190	CP Oct	348772511	1	6.68	6.68	0.01	200.14	2.48	0.13	0.07	1.00	0.08
21553	V465 Per	347570557	1	14.04	14.04	0.00	180.75	0.61	0.04	0.03	2.44	0.04
21985	AS Eri	301407485	1	58.82	59.03	0.00	210.64	1.44	0.03	0.03	1.66	0.03
22541	AD Hor	79611815	1	10.99	10.99	0.02	203.79	0.76	0.03	0.02	0.45	0.03
23728	V376 Per	432049507	1	10.06	10.06	0.02	67.90	0.77	0.08	0.07	1.73	0.07
24550	V479 Tau	459908110	1	13.19	13.23	0.00	152.57	0.44	0.17	0.06	1.34	0.06
24809	V386 Per	94549636	1	18.18	22.33	0.00	63.84	0.09	0.01	0.01	2.50	0.02

Table 2 — continued from previous page

HD	Name	TIC	R2000	f_{cat} d^{-1}	f_1 d^{-1}	a_1 ppt	dist pc	e_dist pc	A_V mag	e_A_V mag	M_V mag	e_M_V mag
26123	V407 Cep	420755646	1	13.57	13.58	0.02	—	—	0.00	0.00	1.96	0.01
26574	38 Eri	67687505	1	13.39	12.23	0.01	38.42	0.22	0.22	0.17	0.90	0.17
26892	UZ Ret	38515566	1	8.14	8.14	0.01	339.81	1.18	0.12	0.06	1.45	0.07
27093	IU Eri	67781014	0	14.51	12.48	0.00	226.69	1.08	0.03	0.02	0.68	0.03
27397	V483 Tau	435910664	1	18.21	17.25	0.00	45.48	0.11	0.06	0.05	2.23	0.05
27459	V696 Tau	435916016	1	27.32	24.77	0.00	47.40	0.24	0.03	0.03	1.84	0.03
27503	BR Hyi	25195864	1	5.00	26.74	0.00	664.38	4.97	0.06	0.05	1.61	0.09
27545	TX Ret	38587180	1	14.93	9.63	0.00	199.33	0.54	0.07	0.04	1.40	0.04
27628	V775 Tau	435923755	1	15.87	13.08	0.00	45.42	0.14	0.09	0.05	2.34	0.05
28052	V777 Tau	60879864	1	5.49	5.18	0.00	46.72	0.48	0.05	0.04	1.08	0.05
28665	EQ Eri	178880326	1	14.29	14.37	0.02	212.39	0.83	0.08	0.05	1.01	0.05
28837	RX Cae	7808834	1	6.49	6.49	0.03	147.51	1.36	0.13	0.08	1.04	0.08
28910	ρ Tau	245860427	1	14.93	15.97	0.00	46.31	0.29	0.03	0.03	1.29	0.03
29870	HS Eri	298981924	0	—	6.89	0.01	124.29	0.37	0.12	0.08	1.15	0.09
30422	EX Eri	589826	1	47.62	48.09	0.00	57.13	0.06	0.04	0.03	2.35	0.03
30600	HV Eri	167486272	1	4.74	4.74	0.02	339.75	2.59	0.06	0.05	0.63	0.06
30716	V1359 Ori	11083205	1	5.49	5.49	0.01	323.51	3.90	0.10	0.06	0.82	0.07
31908	XZ Men	319289587	1	9.23	11.00	0.01	—	—	0.00	0.00	0.30	0.13
32045	S Eri	152373997	1	3.66	3.27	0.00	86.75	0.60	0.06	0.05	0.03	0.06
32846	X Cae	77669416	1	7.40	7.39	0.02	104.70	0.57	0.05	0.05	1.17	0.05
33959	KW Aur	1840666	1	11.35	11.35	0.01	83.24	0.72	0.05	0.05	0.36	0.05
34409	BS Cam	417652271	1	5.54	4.17	0.00	401.04	2.87	0.11	0.06	0.31	0.06
37857	EE Cam	70657495	1	4.93	4.93	0.02	223.94	0.88	0.11	0.09	0.84	0.09
38882	RY Lep	93441696	1	4.44	4.44	0.10	437.06	15.66	0.13	0.11	-0.06	0.13
39244	YY Pic	299884840	1	9.74	9.74	0.02	153.22	0.36	0.04	0.03	1.57	0.03
39996	AA Col	100830119	1	6.66	6.66	0.02	226.17	0.80	0.11	0.07	1.27	0.07
40372	V1004 Ori	282270717	1	16.39	15.31	0.00	106.63	0.37	0.04	0.03	0.71	0.03
40535	V474 Mon	67265166	1	7.35	7.35	0.06	93.82	0.26	0.09	0.07	1.19	0.07
40765	UY Col	143168754	1	5.90	5.90	0.04	474.20	2.46	0.12	0.09	1.05	0.09
42503	AU Col	300114686	0	7.00	5.25	0.00	237.38	0.21	0.05	0.04	0.52	0.04
44958	V435 Car	255548143	1	20.00	20.57	0.00	71.29	0.08	0.03	0.03	2.44	0.03
45311	V456 Aur	144101735	1	7.21	7.21	0.02	187.98	1.41	0.11	0.07	1.36	0.07
50018	OX Aur	21291018	1	6.46	6.80	0.00	147.78	0.93	0.15	0.07	0.11	0.08
52788	V383 Car	279361762	1	8.33	8.91	0.00	303.99	1.08	0.14	0.07	0.86	0.07
54250	V752 Mon	168524254	0	4.32	5.32	0.01	—	—	0.00	0.00	0.95	0.01
55057	V571 Mon	5456605	1	10.00	5.25	0.01	87.49	0.49	0.08	0.05	0.65	0.06
55595	HN CMa	65472324	1	4.00	4.73	0.00	211.84	0.86	0.04	0.02	-0.07	0.03
57167	R CMa	409319605	1	21.28	15.85	0.00	—	—	0.00	0.00	2.55	0.01
58634	V368 Pup	173139593	1	8.67	8.67	0.01	180.87	0.57	0.02	0.02	0.56	0.02
58954	NR CMa	49832986	1	6.02	6.85	0.01	89.97	0.27	0.09	0.05	0.77	0.05
59594	V349 Pup	112484997	1	19.88	19.87	0.01	93.34	0.16	0.02	0.02	2.45	0.02
60302	V344 Gem	247165103	1	8.46	8.46	0.01	185.60	0.81	0.07	0.04	1.62	0.04
62437	AZ CMi	280680714	1	10.49	10.50	0.02	148.81	1.09	0.05	0.03	0.55	0.04
63148	V391 Pup	126928121	0	—	8.73	0.01	—	—	0.00	0.00	0.49	0.01
63874	ET Lyn	39011225	0	5.42	5.42	0.00	213.93	8.51	0.09	0.05	0.66	0.08
64191	AD CMi	266328148	1	8.13	8.13	0.09	451.67	2.90	0.08	0.06	0.97	0.07
64491	DD Lyn	14878438	1	20.41	19.76	0.00	64.93	0.32	0.08	0.04	2.08	0.04
66260	V393 Car	364399376	1	7.08	7.08	0.06	199.66	3.54	0.07	0.05	0.90	0.06
67028	—	452926063	1	19.31	19.32	0.00	431.76	4.37	0.05	0.03	0.59	0.04
67147	CO Lyn	80951366	1	6.11	12.67	0.01	141.61	0.39	0.10	0.06	0.97	0.06
67290	V355 Pup	176152984	1	6.71	7.10	0.01	368.17	2.65	0.05	0.03	0.24	0.04
67390	SZ Lyn	192939152	1	8.30	8.30	0.14	525.06	25.47	0.10	0.09	0.74	0.13
67523	ρ Pup	154360594	1	7.10	7.10	0.02	19.44	0.08	0.13	0.12	1.22	0.12
67852	DE CMi	452982723	0	11.30	11.30	0.01	—	—	0.00	0.00	1.86	0.01
67911	CQ Lyn	81003138	1	8.87	8.87	0.02	196.57	1.57	0.10	0.07	1.40	0.07
69213	AI Vel	81709032	1	8.96	8.96	0.09	100.30	0.17	0.05	0.05	1.52	0.05
69242	CR Lyn	22684612	1	7.59	7.59	0.01	172.91	0.65	0.10	0.07	1.36	0.07
69997	HQ Hya	19566581	1	13.25	11.71	0.00	110.32	0.24	0.12	0.05	0.98	0.05
71297	LM Hya	169051549	1	26.32	26.30	0.00	46.74	1.25	0.09	0.14	2.16	0.15

Table 2 — continued from previous page

HD	Name	TIC	R2000	f_{cat} d^{-1}	f_1 d^{-1}	a_1 ppt	dist pc	e_dist pc	A_V mag	e_A_V mag	M_V mag	e_M_V mag
71935	GU Vel	140349824	1	14.29	15.01	0.00	60.66	0.27	0.04	0.04	1.12	0.04
73857	VZ Cnc	366632312	1	5.61	5.61	0.12	221.97	1.15	0.11	0.07	0.86	0.08
74292	FL Cnc	165859518	1	12.50	13.41	0.00	97.47	0.25	0.05	0.03	2.04	0.03
75654	HZ Vel	190158777	1	11.49	14.34	0.00	71.85	0.09	0.04	0.03	2.05	0.03
75747	RS Cha	323292655	1	12.50	11.62	0.00	98.63	0.18	0.06	0.06	1.06	0.06
77906	—	401744720	0	12.90	12.91	0.07	344.85	7.24	0.09	0.06	1.99	0.08
78422	NT Hya	20042408	1	6.94	6.90	0.01	165.86	0.59	0.09	0.06	1.19	0.06
79185	MP Vel	74528796	1	4.29	7.92	0.00	269.47	1.13	0.10	0.05	0.60	0.06
79439	DD UMa	137648019	1	8.00	25.37	0.00	35.83	0.10	0.03	0.02	2.01	0.03
79781	GG UMa	86232782	1	7.42	7.42	0.02	266.90	1.00	0.12	0.07	1.35	0.07
79889	BE Lyn	56914404	1	10.43	10.43	0.11	251.63	1.31	0.04	0.04	1.76	0.05
80886	—	452464329	0	14.27	14.26	0.02	—	—	0.00	0.00	1.83	0.01
81882	KZ UMa	147893556	1	16.67	14.28	0.00	229.55	0.97	0.06	0.04	1.26	0.04
82620	DL UMa	147574768	1	12.03	13.08	0.01	126.72	0.26	0.10	0.04	1.57	0.04
83041	AK Ant	189569123	1	15.15	14.53	0.00	305.90	2.22	0.08	0.04	1.29	0.05
84712	MT Vel	34156938	1	12.50	13.60	0.01	240.74	1.50	0.08	0.04	0.62	0.05
84800	IX UMa	23969903	1	41.67	36.62	0.00	147.98	0.43	0.05	0.03	1.88	0.04
84948	—	453432481	1	12.82	12.63	0.00	255.19	3.95	0.06	0.04	1.03	0.05
84999	υ UMa	331900366	1	7.54	6.27	0.01	35.67	0.24	0.09	0.08	0.92	0.08
85040	DG Leo	88024537	1	12.11	12.11	0.00	216.27	22.95	0.03	0.03	-0.36	0.18
86301	BF Ant	22234795	0	—	5.03	0.00	143.91	0.47	0.03	0.02	0.49	0.03
87700	V336 Vel	462426434	1	8.27	12.42	0.01	132.24	0.26	0.13	0.06	1.11	0.06
88824	LW Vel	259761784	1	7.98	8.98	0.01	49.67	0.13	0.05	0.04	1.74	0.04
89343	EN UMa	103692670	1	9.09	6.43	0.01	130.07	0.69	0.06	0.04	0.24	0.05
90001	V344 Vel	220628281	1	6.68	6.68	0.01	247.53	1.20	0.08	0.05	0.84	0.05
93044	EO UMa	17329905	1	11.90	11.91	0.02	113.97	0.28	0.06	0.04	1.78	0.04
93137	UX LMi	337319844	1	6.64	6.64	0.02	426.41	10.83	0.11	0.08	0.85	0.09
93142	AZ Ant	54253999	1	9.50	9.50	0.01	256.99	1.41	0.10	0.05	0.73	0.06
93298	V353 Vel	106886169	1	4.04	4.04	0.01	312.77	1.88	0.04	0.03	0.12	0.04
94033	KZ Hya	188209486	1	16.81	16.80	0.22	330.80	7.19	0.11	0.09	2.36	0.11
94480	WW LMi	138738145	0	—	7.88	0.01	130.68	0.55	0.10	0.05	0.51	0.05
94985	IW Vel	120856811	1	6.67	10.15	0.01	108.68	0.26	0.03	0.02	0.69	0.03
95321	V527 Car	304050480	1	4.68	4.68	0.02	531.78	6.11	0.05	0.05	0.42	0.06
97302	FI UMa	302349701	1	25.00	15.95	0.00	104.91	0.22	0.01	0.01	1.51	0.01
98851	LR UMa	144311964	0	18.15	8.97	0.00	152.44	0.54	0.12	0.06	1.38	0.06
99002	CX UMa	17992601	1	10.00	14.80	0.00	148.40	0.54	0.07	0.05	1.01	0.05
99983	HQ UMa	284596378	1	8.65	8.65	0.01	163.82	1.36	0.11	0.05	0.93	0.05
100363	SU Crt	157787615	1	18.18	18.77	0.00	169.76	1.65	0.05	0.04	2.42	0.05
101158	V837 Cen	429143728	1	12.17	10.84	0.01	191.91	0.59	0.06	0.04	0.69	0.04
101696	VY Crt	270265624	1	7.34	7.34	0.03	131.88	2.89	0.12	0.08	1.17	0.09
102355	KW UMa	138590902	1	8.20	15.91	0.00	109.20	0.61	0.12	0.05	1.27	0.05
102480	MX UMa	11891826	0	8.62	16.19	0.01	263.85	0.53	0.11	0.05	1.24	0.05
102541	V1023 Cen	454109915	1	20.00	19.90	0.01	115.78	0.31	0.03	0.02	2.60	0.03
103279	—	293110952	0	14.20	14.21	0.03	421.82	8.48	0.06	0.05	2.71	0.10
104036	EE Cha	454961439	1	33.33	33.87	0.01	104.82	0.26	0.01	0.01	1.63	0.02
104237	DX Cha	357040880	1	33.33	33.28	0.00	106.52	0.43	0.03	0.03	1.43	0.04
104288	OR Dra	142946146	0	8.87	8.86	0.00	206.93	17.00	0.10	0.06	0.73	0.20
104513	DP UMa	141201605	1	25.00	18.07	0.00	—	—	0.00	0.00	2.56	0.04
105058	—	53523744	1	25.00	9.13	0.00	—	—	0.00	0.00	1.28	0.01
105234	EF Cha	357165560	1	18.87	17.95	0.00	—	—	0.00	0.00	2.41	0.01
105513	CO Cru	67533256	1	6.85	6.86	0.01	380.94	1.56	0.10	0.06	1.25	0.06
105759	II Vir	176867792	1	23.64	23.65	0.01	92.69	0.27	0.03	0.02	1.69	0.03
107131	FM Com	328860893	1	15.08	14.93	0.00	85.52	0.20	0.01	0.01	1.77	0.02
107513	KU Com	356702180	1	33.33	19.91	0.00	86.51	0.30	0.04	0.04	2.64	0.04
107904	AI CVn	284593009	1	8.60	5.05	0.02	131.81	1.32	0.10	0.07	0.33	0.07
109585	TU Crv	83207850	1	12.20	10.62	0.00	75.16	1.60	0.14	0.05	1.67	0.06
109663	—	260842067	0	5.36	5.36	0.05	548.38	4.30	0.05	0.04	1.28	0.05
110377	GG Vir	390607729	1	20.00	31.35	0.00	71.65	0.16	0.01	0.01	1.93	0.02
110951	FM Vir	390633441	1	13.91	13.91	0.00	80.45	0.70	0.08	0.06	0.61	0.06

Table 2 — continued from previous page

HD	Name	TIC	R2000	f_{cat} d^{-1}	f_1 d^{-1}	a_1 ppt	dist pc	e_dist pc	A_V mag	e_A_V mag	M_V mag	e_M_V mag
111604	DT CVn	17654683	0	8.77	5.33	0.01	108.70	0.05	0.03	0.02	0.66	0.02
111786	MO Hya	9524429	1	31.06	36.01	0.00	62.09	0.43	0.04	0.03	2.14	0.04
113537	V947 Cen	453750774	1	7.29	7.30	0.01	99.95	0.28	0.12	0.07	1.31	0.07
114042	V950 Cen	253513495	1	6.61	6.61	0.00	258.12	1.66	0.04	0.02	0.67	0.03
114620	V954 Cen	442837381	1	9.14	9.14	0.02	139.80	0.31	0.09	0.07	1.44	0.07
115308	DK Vir	66693422	1	8.61	7.58	0.01	125.16	0.38	0.10	0.05	1.10	0.05
115520	—	105579901	0	18.83	17.77	0.01	292.72	1.16	0.04	0.03	1.06	0.04
115604	AO CVn	180651551	1	8.22	8.22	0.01	78.25	0.64	0.07	0.07	0.17	0.07
116994	V743 Cen	438816206	1	9.78	9.78	0.05	226.64	1.08	0.07	0.06	1.85	0.06
117589	PP Com	368127841	0	16.05	17.72	0.00	106.41	0.03	0.07	0.03	2.17	0.03
117661	HX Vir	32146574	1	23.26	22.27	0.00	83.08	0.22	0.04	0.03	1.36	0.04
118326	LW Mus	342500794	1	6.51	6.51	0.04	375.31	8.82	0.14	0.09	1.21	0.10
118743	BZ Boo	282811788	0	2.70	16.30	0.00	225.58	1.73	0.10	0.04	1.31	0.04
118954	IP UMa	458452969	1	10.00	10.00	0.01	240.65	0.97	0.08	0.04	0.69	0.05
120500	FQ Boo	399182167	1	20.41	21.05	0.00	120.91	0.64	0.01	0.01	1.19	0.02
120635	—	299948201	0	7.08	7.08	0.03	392.93	0.87	0.06	0.06	0.77	0.06
120896	QT Vir	392979958	0	17.79	7.61	0.00	223.10	0.98	0.07	0.04	1.70	0.04
121517	—	241787384	0	9.01	11.01	0.07	300.62	1.26	0.09	0.08	1.93	0.08
123460	V1338 Cen	242302902	0	7.64	7.64	0.12	644.85	8.39	0.10	0.10	1.24	0.11
124675	kap 2 Boo	310362802	1	15.43	15.44	0.00	49.63	0.21	0.04	0.03	1.00	0.03
124953	CN Boo	135169898	1	22.83	11.56	0.00	46.20	0.06	0.04	0.03	2.60	0.03
125081	MX Vir	46041110	1	6.49	6.49	0.01	149.23	0.44	0.15	0.10	1.33	0.10
125161	ι Boo	310381204	1	37.74	36.75	0.00	29.51	0.06	0.03	0.03	2.36	0.03
125162	lambda Boo	168708816	1	43.48	38.17	0.00	30.64	0.12	0.03	0.03	1.71	0.03
126742	—	241843363	0	5.99	5.99	0.05	550.00	3.50	0.16	0.11	0.89	0.12
126859	V853 Cen	290932786	1	18.94	16.31	0.00	140.57	0.25	0.15	0.04	1.09	0.04
127269	MP Hya	83860356	1	29.94	29.65	0.00	180.57	0.97	0.03	0.02	1.47	0.03
127411	IT Dra	166177270	1	23.04	16.85	0.00	139.30	0.32	0.04	0.03	1.76	0.04
127695	V1034 Cen	395108754	1	4.26	4.18	0.00	282.55	1.01	0.13	0.06	1.29	0.06
127711	V1035 Cen	395425079	1	12.50	11.68	0.00	276.62	2.37	0.16	0.04	1.34	0.05
127759	EI Dra	166179291	1	14.79	14.79	0.01	365.20	1.82	0.05	0.03	0.68	0.04
127762	gam Boo	67991192	1	13.70	13.59	0.00	26.29	0.12	0.07	0.05	0.85	0.05
127927	V1036 Cen	396855479	1	9.09	9.47	0.00	486.62	3.05	0.12	0.05	1.06	0.06
127929	ER Dra	166179517	1	11.35	11.38	0.00	122.26	0.33	0.07	0.03	0.77	0.04
128157	V896 Cen	430665759	1	20.00	19.86	0.00	152.75	0.46	0.11	0.05	2.26	0.05
128862	PR Aps	402305954	0	—	10.42	0.01	251.40	1.05	0.13	0.06	0.91	0.07
129041	BT Cir	403779926	1	28.25	28.20	0.00	114.10	0.27	0.03	0.02	2.10	0.02
129494	BO Cir	292435853	1	7.08	8.08	0.00	364.32	1.63	0.18	0.08	1.73	0.08
132209	BV Cir	453848870	1	6.33	6.33	0.01	127.77	0.30	0.10	0.05	0.94	0.05
133194	HY Lib	440958702	1	6.82	6.82	0.03	194.10	1.01	0.13	0.09	1.15	0.09
134185	HU Lup	122932611	1	6.52	7.66	0.01	454.35	2.64	0.11	0.07	0.77	0.07
135383	OP Aps	407012535	1	7.20	7.20	0.02	207.83	0.71	0.09	0.07	1.41	0.07
140436	gam CrB	255861229	0	33.33	4.50	0.00	44.80	0.04	0.06	0.09	0.53	0.10
140639	—	178463456	0	4.95	4.95	0.10	425.87	2.98	0.15	0.12	1.20	0.12
143466	CL Dra	458485558	1	13.11	14.85	0.00	33.78	0.08	0.05	0.04	2.27	0.05
145393	—	382538797	1	31.95	33.61	0.00	251.10	0.33	0.11	0.06	2.76	0.06
148638	NP TrA	402646773	0	16.31	15.30	0.00	251.30	1.35	0.03	0.02	0.87	0.03
149530	V1060 Sco	280816457	1	5.53	5.58	0.01	404.33	2.83	0.15	0.09	0.64	0.09
153747	V922 Sco	346505765	1	21.28	21.47	0.01	177.14	0.69	0.04	0.03	1.14	0.03
153805	V1072 Sco	347028423	1	7.47	7.47	0.01	182.73	1.09	0.09	0.05	0.97	0.06
154225	V929 Her	82551645	1	6.93	6.93	0.01	—	—	0.00	0.00	1.39	0.01
154605	—	43173526	0	9.93	11.94	0.07	285.17	1.18	0.19	0.12	2.13	0.12
154731	MR Dra	274674793	0	31.25	30.26	0.00	207.20	0.23	0.03	0.02	1.59	0.02
155118	V873 Her	143166570	1	7.91	7.86	0.00	240.52	1.61	0.10	0.07	1.40	0.07
155514	V620 Her	257456864	1	11.31	11.32	0.01	80.12	0.11	0.04	0.04	1.63	0.04
158741	V949 Sco	100701385	1	4.61	8.23	0.00	119.66	0.36	0.14	0.07	0.64	0.08
159223	V648 Her	321813050	0	3.45	46.30	0.00	79.24	0.10	0.03	0.03	2.32	0.04
160589	V703 Sco	193310172	1	8.68	8.68	0.07	189.09	0.15	0.10	0.09	1.37	0.09
161032	V352 Pav	306889170	1	9.35	11.82	0.02	110.58	0.29	0.08	0.05	1.21	0.05

Table 2 — continued from previous page

HD	Name	TIC	R2000	f_{cat} d^{-1}	f_1 d^{-1}	a_1 ppt	dist pc	e_dist pc	A_V mag	e_A_V mag	M_V mag	e_M_V mag
161287	V966 Her	256007029	1	7.52	7.52	0.00	212.82	0.69	0.09	0.06	1.25	0.06
168740	V346 Pav	365996589	1	27.78	30.75	0.00	71.12	0.14	0.03	0.02	1.84	0.03
168947	V704 CrA	89975166	1	17.24	14.59	0.00	258.05	1.64	0.06	0.04	1.00	0.05
170625	V668 CrA	91406903	1	11.36	26.56	0.00	298.55	1.41	0.12	0.06	1.22	0.06
173794	V353 Tel	324889453	0	0.31	24.87	0.00	165.15	1.53	0.04	0.06	0.99	0.11
173844	—	359678383	0	15.80	15.78	0.00	178.29	0.36	0.05	0.03	2.34	0.04
173977	HN Dra	232637376	0	8.56	8.56	0.00	236.28	0.86	0.09	0.07	1.12	0.07
176503	V544 Lyr	20816780	1	8.83	8.83	0.00	271.50	1.20	0.07	0.04	0.20	0.04
176723	V701 CrA	254079940	1	7.39	8.94	0.00	65.38	0.21	0.12	0.07	1.53	0.07
177482	sigma Oct	468184895	1	10.31	10.49	0.01	90.07	0.45	0.08	0.05	0.59	0.05
177594	V549 Lyr	42059528	1	7.85	7.85	0.01	285.15	1.44	0.04	0.03	0.77	0.03
178905	—	271523213	0	8.29	8.28	0.01	359.57	29.65	0.09	0.06	0.97	0.19
182634	—	122683109	0	15.04	13.42	0.00	249.51	1.07	0.05	0.03	0.90	0.03
184522	V2084 Cyg	138160886	1	11.36	11.37	0.01	122.89	0.22	0.09	0.05	1.81	0.05
185139	QQ Tel	143463658	1	15.31	15.54	0.01	102.07	0.31	0.06	0.04	1.15	0.04
185332	V1745 Cyg	213679825	1	18.73	25.58	0.00	140.54	0.43	0.04	0.03	1.66	0.03
186357	V1276 Cyg	216982075	1	11.36	12.11	0.00	84.32	0.09	0.17	0.06	1.74	0.06
186786	NZ Pav	339600902	1	12.50	13.71	0.00	59.45	0.15	0.08	0.04	2.08	0.04
187764	CN Dra	258388363	1	10.00	5.05	0.01	173.06	5.93	0.12	0.09	0.02	0.11
188136	CC Oct	346793769	1	8.01	8.01	0.01	193.48	3.58	0.14	0.09	1.40	0.10
188520	CE Oct	313552150	1	18.35	14.09	0.00	141.86	0.48	0.02	0.02	2.23	0.02
191635	V2109 Cyg	294598376	1	5.37	5.38	0.05	212.02	0.68	0.09	0.07	0.78	0.07
191804	IN Dra	269697721	1	7.29	7.29	0.01	217.90	1.22	0.11	0.05	1.20	0.05
191850	—	129277739	1	13.51	13.53	0.02	350.32	5.22	0.12	0.08	1.86	0.09
192518	NU Vul	452310756	1	5.32	5.32	0.01	95.98	0.55	0.04	0.03	0.25	0.03
192640	V1644 Cyg	10988057	1	37.45	37.43	0.01	40.74	0.13	0.04	0.03	1.86	0.03
192871	V383 Vul	304501606	1	5.43	7.39	0.01	199.86	0.67	0.12	0.06	0.54	0.06
193138	IO Dra	403114672	0	—	8.73	0.00	185.71	3.45	0.13	0.07	1.34	0.08
194492	V382 Pav	404239187	1	7.08	7.08	0.05	385.84	1.89	0.07	0.07	0.90	0.07
195961	ρ Pav	351535191	1	8.76	10.31	0.01	62.32	0.37	0.17	0.10	0.72	0.10
196517	V342 Pav	387241049	1	29.41	32.50	0.00	167.70	0.48	0.03	0.04	2.31	0.04
196638	BU Mic	291112607	1	7.22	7.22	0.01	180.92	0.63	0.12	0.06	0.80	0.07
197100	V2129 Cyg	343264872	1	6.46	6.46	0.02	351.17	3.40	0.08	0.06	0.50	0.06
197157	eta Ind	100708841	0	—	30.47	0.00	24.20	0.06	0.04	0.04	2.54	0.04
198830	BQ Ind	354171926	1	12.20	12.20	0.08	362.89	2.34	0.06	0.05	2.00	0.06
199434	V388 Pav	372344502	1	6.32	6.32	0.01	302.80	1.48	0.07	0.06	1.28	0.06
199757	ZZ Mic	126659093	1	14.88	14.89	0.11	331.26	1.85	0.04	0.04	1.81	0.04
199908	DQ Cep	336444537	1	12.69	12.68	0.01	183.71	0.48	0.11	0.06	0.82	0.06
200925	V1719 Cyg	290277380	1	3.74	3.74	0.09	387.29	2.32	0.10	0.08	-0.05	0.09
204615	V2455 Cyg	266794067	0	10.62	10.62	0.13	—	—	0.00	0.00	1.37	0.02
205847	CF Ind	139825582	1	5.92	5.93	0.01	209.65	0.97	0.09	0.04	1.01	0.05
206379	RS Gru	139845816	1	6.80	6.80	0.15	245.74	1.18	0.05	0.05	1.26	0.05
206553	CG Oct	419666736	1	15.87	8.18	0.01	103.72	0.16	0.07	0.04	1.41	0.04
206631	V360 Cep	322202923	1	25.00	57.53	0.00	—	—	0.00	0.00	2.03	0.01
208435	BZ Gru	197686479	1	6.77	8.27	0.01	125.55	0.47	0.11	0.06	0.57	0.06
208664	BE Ind	394015973	1	21.19	21.90	0.00	224.12	1.44	0.04	0.03	1.40	0.03
208999	BX Ind	265566844	1	5.63	5.63	0.03	216.69	0.77	0.10	0.07	1.11	0.07
210111	—	229059574	1	27.78	30.21	0.00	—	—	0.00	0.00	1.91	0.00
211336	ϵ Cep	330608569	1	24.27	12.73	0.00	—	—	0.00	0.00	2.09	0.01
213204	UV PsA	253917376	1	8.77	9.15	0.01	215.40	1.22	0.10	0.06	1.63	0.06
213655	UW PsA	209362175	1	15.38	15.71	0.00	168.40	2.22	0.11	0.05	1.26	0.06
213669	DR Gru	219332123	0	15.02	28.24	0.01	—	—	0.00	0.00	2.16	0.00
214441	CC Gru	161172103	1	8.01	7.94	0.01	119.78	0.28	0.13	0.06	1.13	0.06
217236	WX PsA	89464315	1	8.01	8.01	0.01	95.33	0.63	0.08	0.07	0.52	0.08
219586	V388 Cep	427651165	1	3.68	4.30	0.01	114.92	0.49	0.07	0.05	0.18	0.05
219891	—	173771603	1	10.08	10.08	0.00	137.53	0.59	0.02	0.01	0.80	0.02
220237	V459 Cep	326201430	1	5.59	5.59	0.01	210.54	0.62	0.14	0.06	0.86	0.06
220392	DQ Gru	469933721	1	4.68	4.58	0.01	125.18	0.54	0.06	0.03	0.57	0.04
220978	BS Scl	303584611	1	8.48	17.63	0.00	127.19	0.34	0.08	0.04	1.31	0.04

Table 2 — continued from previous page

HD	Name	TIC	R2000	f_{cat} d^{-1}	f_1 d^{-1}	a_1 ppt	dist pc	e_dist pc	A_V mag	e_A_V mag	M_V mag	e_M_V mag
221142	V377 Cep	461545977	1	13.70	15.34	0.01	123.95	0.24	0.05	0.04	1.11	0.04
221756	V340 And	333375443	1	22.73	22.26	0.00	76.63	0.25	0.07	0.04	1.08	0.05
223065	SX Phe	224285325	1	18.18	18.19	0.14	—	—	0.00	0.00	2.72	0.00
223338	BS Aqr	9632550	1	5.06	5.05	0.11	528.98	10.56	0.09	0.08	0.66	0.09
223480	BF Phe	144387364	1	16.03	16.02	0.00	107.13	0.22	0.05	0.03	2.22	0.03
223661	V396 And	177363174	1	9.55	9.55	0.01	216.87	1.49	0.15	0.06	1.03	0.07
224852	—	355687188	0	8.19	8.19	0.07	584.00	6.92	0.10	0.07	1.02	0.08
227695	V1821 Cyg	90350726	1	9.24	8.82	0.01	607.06	7.91	0.12	0.07	0.95	0.09
230990	V336 Sge	343216782	1	5.43	6.22	0.01	474.43	5.92	0.10	0.07	0.82	0.08
234366	V927 Her	274510661	1	7.66	7.66	0.03	—	—	0.00	0.00	1.33	0.01
254061	—	166979292	0	13.33	17.22	0.08	349.58	2.67	0.05	0.05	2.36	0.07
261331	V588 Mon	220249462	1	7.14	5.14	0.00	578.77	5.33	0.05	0.03	0.91	0.06
261446	V589 Mon	220281554	1	6.27	6.49	0.01	620.57	5.24	0.14	0.08	0.90	0.08
290764	V1247 Ori	11199521	1	10.31	10.32	0.01	401.20	2.77	0.05	0.04	1.75	0.06
290799	V1790 Ori	11361473	0	23.53	22.53	0.00	420.68	3.75	0.05	0.03	2.50	0.08
292962	—	33149129	0	9.19	9.19	0.07	486.18	3.75	0.06	0.05	1.41	0.06
316092	V974 Oph	200624064	1	5.23	5.23	0.07	1088.42	73.67	0.28	0.17	1.04	0.27
339660	V381 Vul	245151597	1	17.86	10.43	0.00	814.38	28.26	0.06	0.06	0.56	0.10
341555	V979 Her	135362719	1	8.65	8.65	0.01	230.41	0.81	0.08	0.06	1.56	0.06
—	AB Cas	354922610	1	17.15	17.16	0.01	329.74	1.47	0.11	0.10	2.59	0.11
—	AE UMa	357132618	1	11.63	11.62	0.14	735.57	16.08	0.09	0.07	1.93	0.12
—	AI Hya	455178154	1	7.25	6.24	0.00	611.24	6.20	0.12	0.07	0.31	0.07
—	AN Lyn	56882581	1	10.17	10.17	0.05	666.20	10.31	0.09	0.07	1.44	0.09
—	BO Lyn	99091734	1	10.71	10.71	0.06	1343.42	29.97	0.06	0.06	0.79	0.15
—	CC And	191466237	1	8.01	8.00	0.04	379.57	2.26	0.08	0.07	1.37	0.07
—	DE Lac	119486942	1	3.94	4.00	0.03	765.00	10.25	0.17	0.12	0.75	0.12
—	ES Cir	298112357	0	9.84	9.85	0.17	595.38	5.16	0.12	0.10	1.96	0.12
—	GP And	436546358	1	12.71	12.71	0.16	545.24	7.66	0.09	0.08	2.03	0.13
—	GP Cnc	458658640	0	8.84	11.77	0.01	—	—	0.00	0.00	2.04	0.20
—	GW Dra	329153513	1	7.92	7.92	0.02	358.69	2.04	0.10	0.07	1.40	0.08
—	GW UMa	150276417	0	4.92	4.92	0.12	676.48	21.37	0.20	0.13	0.34	0.14
—	OS Gem	171300396	1	15.48	14.50	0.00	453.16	2.79	0.04	0.03	1.06	0.04
—	UV Tri	61275530	1	10.00	9.33	0.01	710.73	15.91	0.08	0.06	1.81	0.12
—	V1162 Ori	34512862	1	12.71	12.71	0.04	444.01	4.65	0.08	0.07	1.67	0.08
—	V1199 Ori	43846109	0	—	13.03	0.00	608.61	6.48	0.10	0.05	2.69	0.21
—	V1232 Cen	181087723	0	—	7.72	0.11	1450.15	25.54	0.11	0.09	1.33	0.10
—	V402 Cep	468294062	1	8.14	8.13	0.01	630.06	4.41	0.15	0.09	1.40	0.10
—	V420 Car	364398340	0	—	16.03	0.00	423.76	8.31	0.07	0.04	2.18	0.05
—	V421 Car	364398097	0	—	39.12	0.00	411.41	1.82	0.05	0.03	2.75	0.03
—	V459 Per	259254245	1	27.03	22.48	0.00	174.82	0.44	0.11	0.05	2.86	0.05
—	V593 Lyr	289325437	0	11.36	9.79	0.18	1459.59	25.88	0.09	0.07	0.77	0.19
—	V673 Hya	168384036	0	9.25	9.25	0.11	576.54	7.62	0.09	0.08	1.73	0.10
—	V798 Cyg	69546708	1	5.13	5.13	0.14	2450.28	51.23	0.09	0.07	0.96	0.08
—	V830 Her	308407544	1	5.56	5.65	0.03	466.45	2.58	0.12	0.09	0.82	0.09
—	V871 Cas	252046615	1	7.71	7.71	0.03	—	—	0.00	0.00	1.32	0.02
—	VX Hya	289711518	1	4.48	4.48	0.09	932.72	12.68	0.07	0.07	0.68	0.11
—	XX Cyg	233310793	1	7.41	7.42	0.23	1162.39	20.23	0.11	0.09	1.43	0.19
—	XX Pyx	37366830	1	38.17	38.11	0.01	703.30	13.90	0.06	0.04	2.21	0.06
—	Y Cam	441598163	1	15.04	15.05	0.00	799.37	6.46	0.09	0.10	1.00	0.10
—	YZ Boo	233465540	1	9.61	9.61	0.11	585.02	4.71	0.06	0.05	1.62	0.07
—	—	13972612	0	9.60	10.61	0.00	1778.09	26.62	0.22	0.10	-0.49	0.13
—	—	46937596	0	7.89	7.89	0.07	811.80	10.99	0.09	0.08	1.54	0.15
—	—	60405689	0	14.99	14.99	0.06	567.84	5.83	0.08	0.06	2.48	0.11
—	—	65138566	0	18.35	18.33	0.03	538.03	5.08	0.06	0.05	2.48	0.10
—	—	78850814	0	9.12	9.12	0.07	1099.34	10.85	0.15	0.11	1.25	0.17
—	—	90185615	0	7.20	7.20	0.06	578.33	5.45	0.13	0.12	1.63	0.14
—	—	90322352	0	9.33	9.33	0.10	1074.32	29.73	0.08	0.08	1.29	0.17
—	—	120857354	0	20.49	20.49	0.04	—	—	0.00	0.00	2.46	0.01
—	—	130474019	0	—	12.28	0.12	975.66	10.18	0.08	0.07	2.20	0.22

Table 2 — continued from previous page

HD	Name	TIC	R2000	f_{cat} d^{-1}	f_1 d^{-1}	a_1 ppt	dist pc	e_dist pc	A_V mag	e_A_V mag	M_V mag	e_M_V mag
—	—	142945544	0	16.47	18.48	0.07	463.26	9.86	0.05	0.05	2.40	0.09
—	—	148357344	0	—	11.10	0.14	1229.90	21.70	0.15	0.11	1.51	0.28
—	—	155128092	0	—	14.68	0.10	775.74	12.54	0.06	0.05	1.90	0.11
—	—	178616716	0	—	9.76	0.09	1224.71	23.01	0.11	0.10	1.43	0.10
—	—	183532876	0	5.98	5.98	0.16	—	—	0.00	0.00	0.95	0.05
—	—	261089835	0	7.15	11.16	0.08	1226.34	28.75	0.14	0.11	1.32	0.21
—	—	262652067	0	5.63	5.63	0.06	726.83	5.89	0.15	0.11	1.37	0.13
—	—	264482621	0	18.80	18.78	0.04	392.61	2.46	0.08	0.09	2.71	0.13
—	—	278003738	0	8.55	8.55	0.02	560.78	4.72	0.09	0.07	1.89	0.11
—	—	308396022	0	13.21	13.20	0.07	600.99	10.85	0.10	0.09	2.01	0.13
—	—	308456254	0	6.28	6.28	0.04	706.94	11.11	0.11	0.09	1.57	0.12
—	—	337437469	0	7.62	7.62	0.03	725.73	5.51	0.11	0.11	1.60	0.11
—	—	339675323	0	7.45	7.45	0.06	936.41	18.04	0.16	0.12	1.58	0.19
—	—	349972148	0	5.93	5.93	0.04	—	—	0.00	0.00	1.37	0.02
—	—	358502706	0	11.67	11.67	0.08	984.78	11.30	0.08	0.06	1.73	0.07
—	—	360736543	0	6.71	6.71	0.05	1393.52	29.54	0.08	0.07	0.82	0.14
—	—	362384415	0	—	7.22	0.13	1161.49	30.53	0.11	0.09	1.68	0.22
—	—	374753270	0	7.25	7.25	0.15	733.07	4.85	0.12	0.11	1.61	0.11
—	—	391474560	0	—	10.54	0.09	1122.74	11.83	0.10	0.08	1.70	0.24
—	—	393420032	0	6.01	6.01	0.06	1204.71	25.86	0.15	0.10	0.69	0.13
—	—	410038602	0	—	13.07	0.06	1163.57	23.90	0.06	0.05	1.92	0.21
—	—	431589510	0	—	7.73	0.08	1356.52	138.29	0.10	0.09	1.60	0.31
—	—	453717216	0	8.35	8.35	0.02	—	—	0.00	0.00	2.31	0.01

This paper has been typeset from a TEX/LATEX file prepared by the author.